LA-UR-95- 697

Conf-9411204--1

Los Alamos National Laboratory is operated by the University of California for the United States Department of Energy under contract W-7405-ENG-36.

TITLE: FISSION PROPERTIES OF THE HEAVIEST ELEMENTS

AUTHOR(S): Moller, Peter*§¶
Nix, Ray, T-2

*Japan Atomic Research Institute, Tokai, Naka-gun, Ibaraki, 319-11 Japan

§Center for Mathematical Sciences, University of Aizu, Aizu-Wakamatsu, Fukushima 965-80, Japan

¶Theoretical Division, Los Alamos National Laboratory, Los Alamos, NM 87545

SUBMITTED TO: For publication in the proceedings. Presented at the Dai 2 Kai Hadoron Tataikei no Simulation Symposium, Tokai-mura, Ibaraki, Japan, November 30- December 2, 1994.

Fission properties of the heaviest elements

Peter Möller†‡§¶ and J. Rayford Nix¶

†Japan Atomic Research Institute, Tokai, Naka-gun, Ibaraki, 319-11 Japan

‡Center for Mathematical Sciences, University of Aizu, Aizu-Wakamatsu, Fukushima 965-80, Japan

§P. Moller Scientific Computing and Graphics, Inc., P. O. Box 1440, Los Alamos, NM 87544, USA

¶Theoretical Division, Los Alamos National Laboratory, Los Alamos, NM 87545, USA

Abstract. We discuss fission properties of the heaviest elements. In particular we focus on stability with respect to spontaneous fission and on the prospects of extending the region of known nuclei beyond the peninsula of currently known nuclides.

1. Introduction

The number of elements is limited because nuclei become increasingly unstable with respect to spontaneous-fission and α decay as the proton number increases. Uranium with 92 protons is the last element that occurs in appreciable quantities on earth, because its half-life with respect to spontaneous fission is sufficiently long in relation to the age of the solar system, so that a substantial portion of the uranium originally present on earth still has not decayed. However, as the proton number increases the spontaneous-fission half-lives rapidly decrease: between thorium and the heavy fermium isotopes the decrease is 30 orders of magnitude, with ^{258}Fm having a spontaneous-fission half-life of 0.37 ms.

In the mid 1960s it was suggested that nuclei in the vicinity of the next doubly magic nucleon configuration, namely proton number $Z = 114$ and neutron number $N = 184$ would have their stability sufficiently enhanced to be observable. Some calculations predicted half-lives of the order of 10^9 y for the most stable nucleus ^{294}110 in this region. Nuclei between this "superheavy island" and the end of the peninsula of elements known at the time were thought to be far too short-lived to be observable. Many experimental attempts, all unsuccessful, were made to reach nuclei in the vicinity of the superheavy island.

Since the initial predictions of the existence of an island of relatively stable superheavy elements separated by a sea of instability from the known elements were made, we have come to understand that the situation is much more complex and that there are important modifications to the original ideas.

We discuss here briefly our current picture of the spontaneous-fission properties of the heaviest elements. We also discuss the stability with respect to other decay modes. A more extensive discussion may be found in our recent review article [1]. A very recent development, occurring after the publication of the review article is the discovery of element $Z = 110$ a few weeks before the date of this conference and of element $Z = 111$ a few weeks after the conference.

2. Bimodal Fission

We now know that the short spontaneous-fission half-lives of the heavy Fm isotopes are due not only to the high proton number but also to the onset of a new fission mode: division into symmetric, spherical fission fragments with high kinetic energies. For a long time experimental studies of spontaneous-fission properties showed gradual, predictable changes of such properties as spontaneous-fission half-lives and mass and kinetic-energy distributions as the region of known nuclei above uranium expanded. At the same time evidence started to accumulate that there were rapid changes in fission properties in the heavy fermium region. The first observation of the onset of symmetric fission at the end of the periodic system was a study [2] of ^{257}Fm fission. For ^{258}Fm the changes are even more dramatic. Fission becomes symmetric with a very narrow mass distribution, the kinetic energy of the fragments is about 35 MeV higher than in the asymmetric fission of ^{256}Fm and the spontaneous-fission half-life is 0.37 ms, compared to 2.86 h for ^{256}Fm. The fission-fragment mass distributions and kinetic-energy distributions of ^{258}Fm and four other heavy nuclei are shown in fig. 1, taken from ref. [3], where these experimental results are more extensively discussed. An important feature of some of the kinetic-energy distributions is that the shape is not Gaussian. Instead, some of the distributions are best described as a sum of two Gaussians. For ^{258}Fm, for example, the kinetic-energy distribution can be represented by two Gaussians centered at about 200 and 235 MeV.

The first calculation that showed pronounced multi-valley structure *and* calculated the corresponding spontaneous-fission half-lives was performed in refs. [4,5]. An improved model that also included odd nuclei was presented somewhat later [6]. These calculations determined the potential energy for a set of nuclear shapes leading from the nuclear ground state to both elongated scission configurations ("old valley") and compact two-touching-sphere scission configurations ("new valley"). The shapes are shown in fig. 2. In fig. 3 we show the calculated nuclear potential energy of deformation corresponding to these shapes, for the nucleus ^{258}Fm. Since the appearance of a contour diagram is strongly dependent on the particular variables in terms of which it is displayed it is normally best to avoid displaying the calculated results in terms of the parameters of the actual parameterization. Instead it is best displayed in terms of parameters that characterize the shape in a more general way. One possible choice would be to display the contour diagram in terms of the multipole moments of the shape. However, then the inertia of two separated fragments

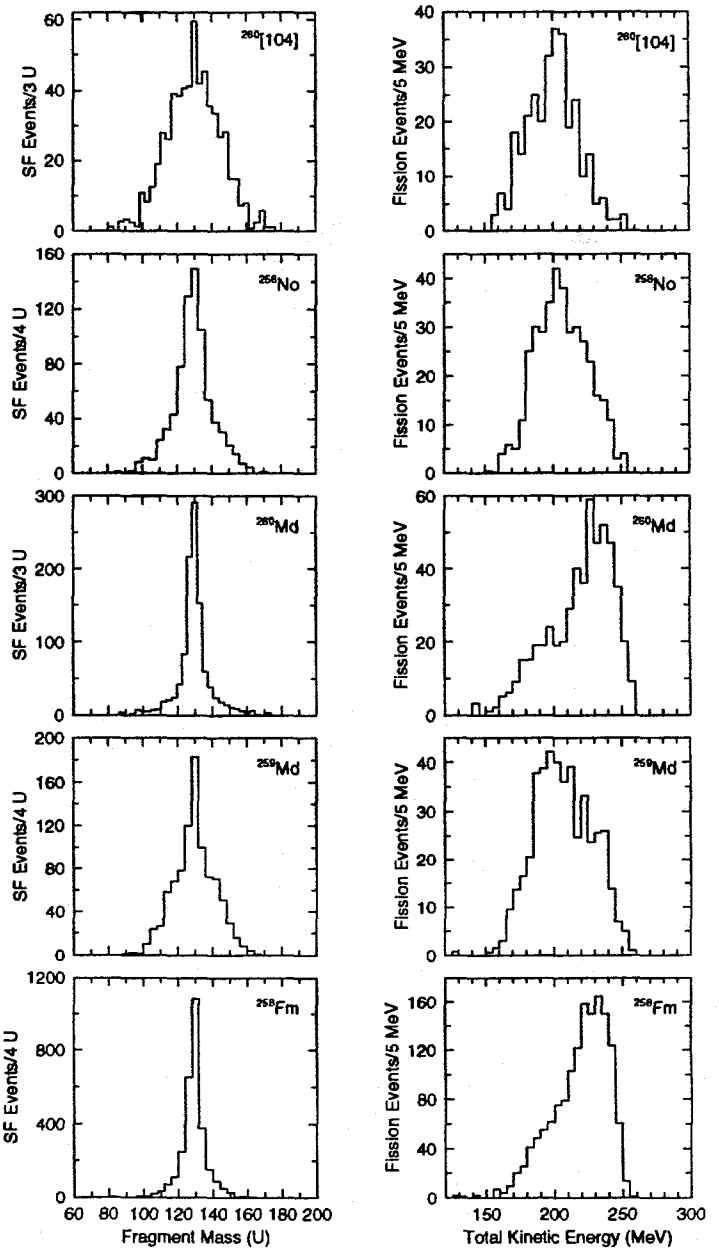

Figure 1. Experimental fission-fragment mass and kinetic-energy distributions for the fission of nuclei close to ^{264}Fm, whose symmetric fragments are doubly magic. The structures of these distributions reflect the valleys, ridges, minima and saddle points of the underlying nuclear potential-energy surfaces.

would not be constant, which would complicate the interpretation of fission potential-energy surfaces. Therefore we have often chosen to display calculated potential-energy surfaces in terms of the two moments r and σ [6,7], where r is the distance between the centers of mass of the two halves of the system and σ is the sum of the root-mean-square extensions along the symmetry axis of the mass of each half of the system about its center of mass.

In fig. 3, there are arrowed lines showing three paths whose significance we now discuss. Most of the fission events will follow the short-dashed path leading into a new

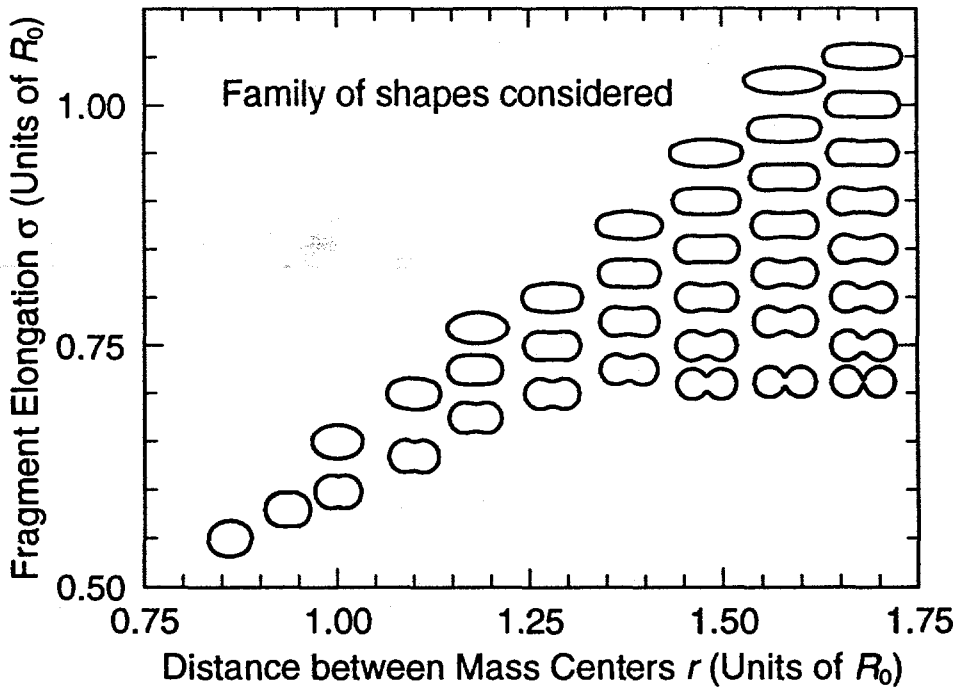

Figure 2. Nuclear shapes for which fission potential-energy surfaces are calculated. The selected shapes allow fission both into compact spherical fragments with high kinetic energies and elongated fragments with normal kinetic energies.

fission valley. There is a *switchback* path leading from a point along the new path across a saddle at about $r = 1.50$, $\sigma = 0.85$ back to the old valley. This switchback path according to our interpretation is responsible for the few low-kinetic-energy events that are observed for this nucleus. The *old* fission path, shown as a dot-dashed line, is not involved at all in the fission process according to our current interpretation.

However, since the saddle along the switchback path in fig. 3 is 3 MeV higher than the outer saddle in the new valley one may conclude that access to the old valley is almost completely blocked by the ridge. On the other hand, one may suspect that mass-asymmetric shape degrees of freedom may lower the saddle along the switchback path.

To investigate this possibility we have calculated the potential energy for a full three-dimensional grid for a choice of shapes that include the switchback saddle and the outer saddle along the new fission valley. From a study of the full three-dimensional results we have determined that the outer saddle along the new fission path at about $r = 1.6$, $\sigma = 0.75$ is not lowered by mass asymmetry, but that the saddle on the switchback path is indeed lowered so that it becomes approximately equal in height to the outer saddle in the new valley.

From the above discussion we conclude that the mechanism behind the bimodal fission process remains the one proposed in our earlier study [4]. Earlier it was thought that the two modes of fission penetrated two completely different barriers. Since, at that time only the ground state was thought to be the same for the two modes it was difficult to understand how the penetrability through two almost uncorrelated barriers could be the same to within about a factor of ten. Our results above resolve this paradox. For ^{258}Fm, fission initially proceeds along the new fission valley, with most events penetrating the

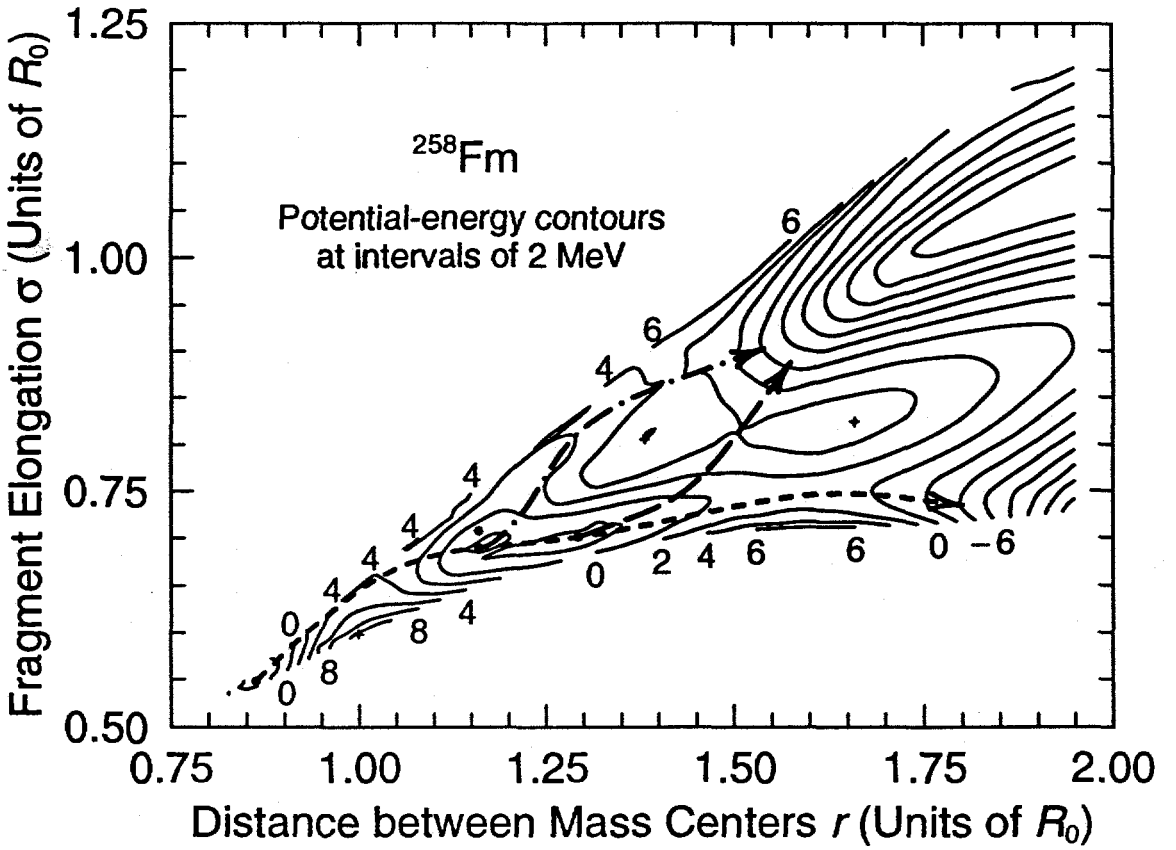

Figure 3. Calculated potential-energy surface for ^{258}Fm [6] for symmetric deformations.

outer saddle along this path. However, a small number of events branch off from the new valley to the saddle along the switchback path and penetrate into the old fission valley. An important point made in our earlier study [4] is that because the barriers leading into the new and old valleys are the same from the ground state to the exit point at the end of the barrier, *except for a tiny portion at the end of the barrier*, it is possible for the branching ratio to be about unity, as is also observed experimentally.

3. Spontaneous-fission half-lives

In a one-dimensional WKB spontaneous-fission model the fission half-life is connected to the penetrability by [8,9]

$$T_{\rm sf} = 10^{-28.04}\ {\rm y}/P \tag{1}$$

where the value $\omega_0 = 1$ MeV$/\hbar$ is used for the frequency of assaults on the barrier. The probability P of penetrating the barrier $V(r)$ at the energy E_0 is given by [10]

$$P = \frac{1}{1+e^K} \tag{2}$$

where

$$K = 2\int_{r_1}^{r_2} \left\{ \frac{2B_r(r)}{\hbar^2}\left[V(r) - E_0\right] \right\}^{1/2} dr \tag{3}$$

Here $V(r)$ is the barrier energy along the selected path. The penetration energy E_0 is the ground-state energy, which includes the zero-point energy in the fission direction at the ground state.

The function $B_r(r)$ is the inertia with respect to r associated with motion in the fission direction. An important aspect of our semi-empirical approach is to deduce asymptotic properties of the semi-empirical inertia from model-independent arguments about the expected general properties of the inertia at both large and small values of r. At large distances we expect $B_r(r)$ to approach the value $\frac{1}{4}M$ appropriate to separated symmetric fragments. At small values or r the inertia is expected to be considerably higher than the hydrodynamical irrotational-flow result, due to microscopic quantum-mechanical effects associated with single-particle level crossings. In our semi-empirical model these asymptotic constraints are taken into account by relating the inertia B_r to the inertia $B_r^{\rm irr}$ corresponding to irrotational flow by [9]

$$B_r - \mu = k(B_r^{\rm irr} - \mu) \tag{4}$$

where k is a semi-empirical constant and μ is the reduced mass of the final symmetric fragments. The parameter k accounts for the increase of the inertia above the hydrodynamical value.

More extensive discussions on the calculation of spontaneous-fission half-lives have been presented elsewhere [1,6], where also calculated spontaneous-fission half-lives are presented. Those studies indicate that the mechanism behind the short spontaneous-fission half-lives of the heavy Fm isotopes is the opening up of the new fission valley leading to compact scission shapes. In this new valley the inertia is considerably lower that in the old valley and it is this feature that is a major contributor to the short spontaneous-fission half-lives. In this valley the outer fission saddle-point height also decreases very rapidly as more neutrons are added, by about 1 MeV for each neutron added, in the vicinity of ^{258}Fm. However, in our calculation for ^{258}Fm the outer saddle is still higher in energy than the ground state.

It is clear that accurate calculations of spontaneous-fission half-lives are difficult, since they are exponentially sensitive to changes in the barrier height, inertia and path length. It is important realize that uncertainties in the ground-state energy influence much more the accuracy of calculated spontaneous-fission half-lives than do uncertainties in calculated saddle-point energies. Figure 4 illustrates this point. A change in the calculated saddle-point height only gives rise to a small, local change in the area under the barrier, whereas a change in the calculated ground-state energy results in a much larger global change. As a rule-of-thumb one can expect that a 1 MeV change in a saddle-point energy results in a one-order-of-magnitude change in the spontaneous-fission half-life whereas a 1 MeV change in a ground-state energy results in a six-order-of-magnitude change. Because ground-state energies influence spontaneous-fission half-lives to such a high degree we discuss in the next section calculated ground-state microscopic corrections

4. Ground-state microscopic corrections, new elements, and α-decay Q values

In fig. 5 we present calculated microscopic corrections for heavy nuclei. The contour lines are spaced at intervals of one MeV. The saddle-point region between ^{208}Pb and the

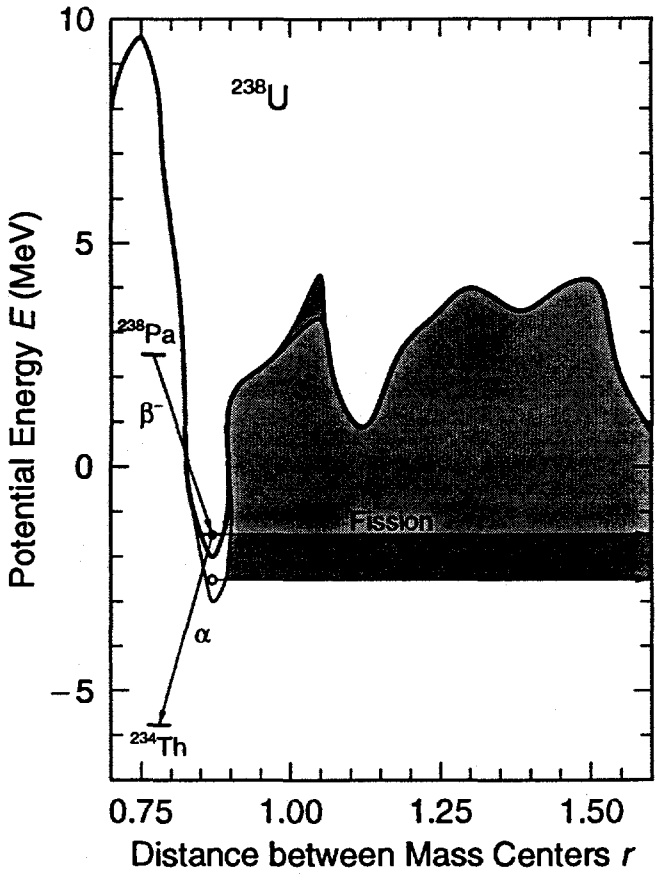

Figure 4. Calculated fission barrier for ^{238}U (thick line). From the ground-state, indicated by a black dot, the nucleus may either fission in a tunneling process through the barrier or decay by α-decay. The area under the barrier is closely related to the calculated spontaneous-fission half-life. Effects of 1 MeV changes in the ground state energy and/or the energy of the first peak are indicated by thinner lines and darker shaded areas. Changes in ground-state energy are much more important than changes in saddle-point energies.

actinide region is just above 0 MeV.

Minima in contour diagrams of calculated microscopic corrections are usually associated with pairs of magic neutron and proton numbers. Thus, in the lower-left-hand corner of the diagram we see a minimum below −10 MeV, corresponding to the doubly magic nucleus $^{208}_{82}\mathrm{Pb}_{126}$. In the upper-right-hand corner of the figure is another minimum at proton number $Z = 115$ and neutron number $N = 179$, at an energy of −9.44 MeV. At $Z = 114$ and $N = 179$ the energy is almost the same. This minimum is located in the region of superheavy elements (SHEs). Beyond $N = 126$ the deepest microscopic correction obtained here does not occur at $Z = 114$, $N = 184$, which is obtained in most older calculations [8,9,11–13], but agrees with earlier results [14] obtained in macroscopic-microscopic calculations based on the folded-Yukawa single-particle potential with the same spin-orbit and diffuseness parameters that are used here. Although the deepest microscopic correction is obtained at $N = 184$ in calculations based on the Woods-Saxon potential, the microscopic correction is almost constant in the interval between $N = 178$ and $N = 184$ [14], and is very similar to that obtained here.

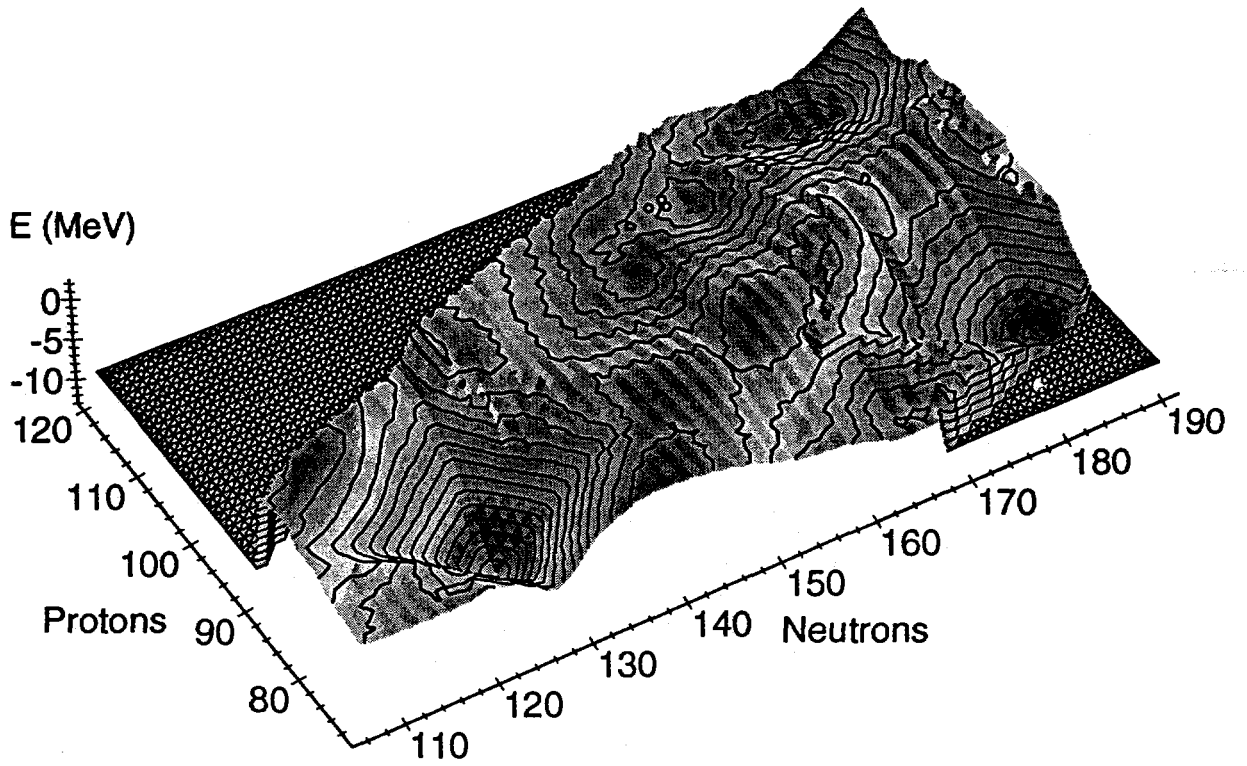

Figure 5. Calculated microscopic corrections for heavy nuclei, plotted versus neutron and proton number.Of special interest is the local minimum centered at $^{272}_{109}\mathrm{Mt}_{163}$, corresponding to *deformed* nuclei of unusual stability. Three black circles slightly to the left of this local minimum indicate 3 isotopes of two new elements, discovered at the GSI in November and December of 1994.

The most stable nucleus in the SHE region does not correspond to the position of the minimum in the microscopic correction but is instead determined by the balance between α decay, β decay and spontaneous fission.

The structure of fig. 5 shows that the contours are not diamond-like around the minimum in the SHE region. Instead, there is a peninsula of stability extending from the superheavy island toward the region of known heavy elements. On this peninsula there is a "rock" of increased stability centered at $Z = 109$, $N = 163$. These structures were partially visible in the 1981 mass calculation [15,16] and fully visible in later work [14]. Similar structures are also present in Woods-Saxon calculations [17]. The rock of stability corresponds to gaps in the level spectra at *deformed* shapes. The unusual stability with respect to spontaneous-fission of $^{252}_{100}\mathrm{Fm}_{152}$ is associated with similar gaps in the single-particle level spectra, again at *deformed* shapes. However, in the contour diagram in fig. 5 these gaps are not manifested as a minimum but instead as a plateau

When superheavy elements were first considered it was thought that they could be reached only by leaping across a sea of instability to regions close to the center of the superheavy region. However, instead of a jump across a sea of instability, the presence of the peninsula of stability extending towards the actinides from the center of the superheavy region has allowed the gradual extension [18–21] of the region of known elements in recent years. Very recently two new elements with proton number $Z = 110$ and proton number $Z = 111$ were observed for the first time. The unambiguous identification was based

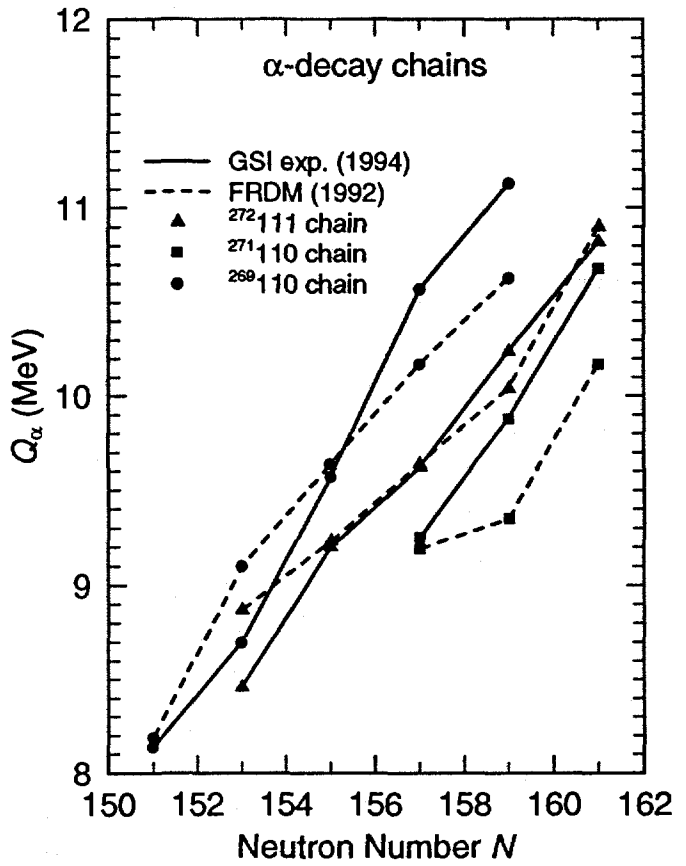

Figure 6. Comparison between Q_α values obtained in the FRDM (1992) and recent experimental data. When several Q values were measured we choose for the figure the highest Q value.

on several observed alpha-decay chains in a position-sensitive detector. Of element 110 both ^{269}110 [20] and ^{271}110 [22] were observed. One isotope, ^{272}111 [21], was observed of element 111. It is of interest to compare these new results with model predictions, made before these experimental results were obtained in November and December of 1994.

In fig. 6 we compare these recently observed α-decay Q values with results of the FRDM (1992) [23,24]. In the FRDM (1992) the error in Q_α is 0.625 MeV, but lower, about 0.5 MeV, if the lighter region of nuclei is excluded [23,24]. It is clear that the average discrepancy in the newly observed chains are well within this stated model error. Actually no error is much larger than 0.5 MeV and several are smaller.

In fig. 7 we compare the experimental results for the ^{272}111 α-decay chains with predictions obtained in the FRDM (1992) [23,24], ETFSI-1 (1992) [25], and FDSM (1990) [26]. Clearly the FRDM (1992) predictions agree much better with data than do the other two models. Because the FRDM (1992) Q_α error is about 0.5 MeV for heavy nuclei, one should not consistently expect this good agreement with new data. However, the overall agreement between the FRDM (1992) and new data for the three chains in fig. 6 confirms the conclusion reached earlier both by simulation [23] and by comparisons with new data [24] that the FRDM (1992) is reliable in the superheavy region, to its stated accuracy.

Nuclei near $Z = 100$ and/or $N = 164$ can divide into fragments with near-magic proton and/or neutron number, which is the reason for the short spontaneous-fission half-

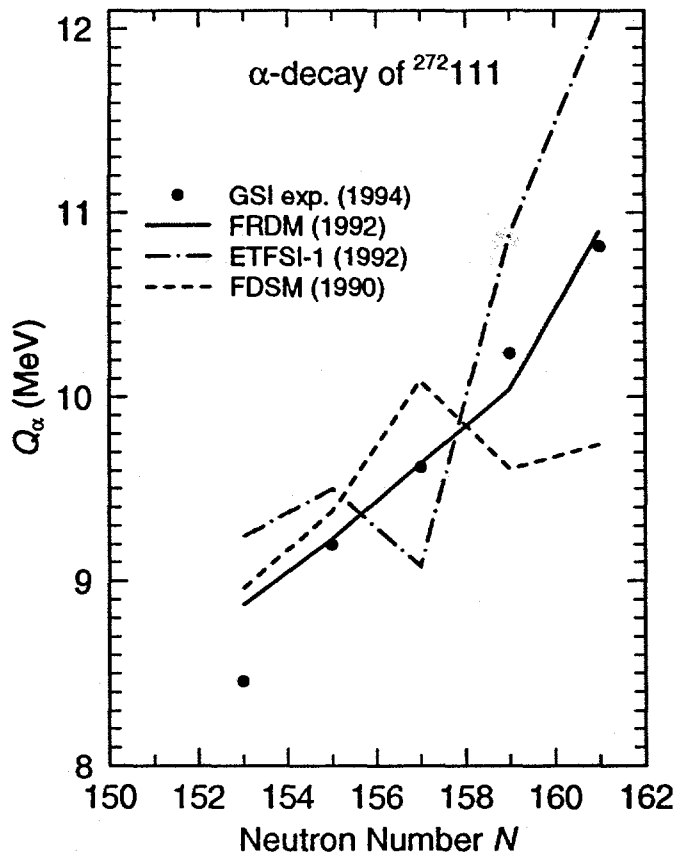

Figure 7. Comparison between Q_α values obtained in the FRDM (1992), ETFSI-1 (1992) and FDSM (1990) models and recent experimental data. When several Q values were measured we choose for the figure the highest Q value.

lives of the neutron-rich Fm isotopes. The rock of stability, in the region of the recently discovered new elements, is near $N = 164$ the magic-fragment neutron shell. This shell has a destabilizing effect because it lowers the outer part of the barrier *and* the inertia. Therefore there has been some discussion whether the stabilizing influence of the rock of stability, which influences the ground state of the fission barrier is sufficient to yield observable decay rates and to make α decay the dominating decay mode. Lower-estimate calculations of the spontaneous-fission half-lives in this region had yielded some spontaneous-fission half-lives in the millisecond range, so spontaneous fission could conceivably compete with α-decay. However, the recent data on element 110 and 111, and data on very neutron-rich isotopes of element 106 [27] has answered the above question: the rock of stability does sufficiently enhance the ground-state shell correction over the destabilizing influence of $N = 164$, so that α-decay is the dominating decay mode.

5. Conclusions

In the vicinity of $Z = 110$ and $N = 162$ *deformed* gaps in nuclear single-particle level spectra yield large, negative microscopic corrections. These ground-state effects stabilize the nucleus with respect to spontaneous fission and α decay. Although the isotopes of these elements that were produced had about 25 less neutrons than the conventional

superheavy island, it has been suggested that the term superheavy is still applicable to these nuclei [18,28], because their liquid-drop barrier is close to zero and their existence comes from an enhanced binding of more than 5 MeV due to *deformed* shells at $Z = 110$ and $N = 162$.

The decay properties of these new nuclei were predicted to within anticipated accuracy by FRDM model calculations. However, there is a need to enhance the accuracy of spontaneous-fission half-life calculations. In particular there is a need for a consistent description of nuclear fission properties from the lightest actinides to the superheavy region within a single model framework. In particular it is necessary to develop a microscopic model for the nuclear inertia that accurately accounts for its variation along the various fission paths shown in fig. 3, its variation between the paths and its variation between nuclei from the actinide to the superheavy region.

This work was supported by the U. S. Department of Energy and by the Japan Atomic Energy Research Institute.

References

[1] P. Möller and J. R. Nix, J. Phys. G: Nucl. Part. Phys. **20** (1994) 1681.

[2] J. P. Balagna, G. P. Ford, D. C. Hoffman, and J. D. Knight, Phys. Rev. Lett. **26** (1971) 145.

[3] E. K. Hulet, J. F. Wild, R. J. Dougan, R. W. Lougheed, J. H. Landrum, A. D. Dougan, M. Schädel, R. L. Hahn, P. A. Baisden, C. M. Henderson, R. J. Dupzyk, K. Sümmerer, and G. R. Bethune, Phys. Rev. Lett. **56** (1986) 313.

[4] P. Möller, J. R. Nix, and W. J. Swiatecki, Nucl. Phys. **A469** (1987) 1.

[5] P. Möller, J. R. Nix, and W. J. Swiatecki, Proc. Int. School-Seminar on heavy ion physics, Dubna, USSR, 1986, JINR Report JINR-D7-87-68 (1987) p. 167.

[6] P. Möller, J. R. Nix, and W. J. Swiatecki, Nucl. Phys. **A492** (1989) 349.

[7] P. Möller and J. R. Nix, Nucl. Phys. **A272** (1976) 502.

[8] S. G. Nilsson, C. F. Tsang, A. Sobiczewski, Z. Szymański, S. Wycech, C. Gustafson, I.-L. Lamm, P. Möller, and B. Nilsson, Nucl. Phys. **A131** (1969) 1.

[9] E. O. Fiset and J. R. Nix, Nucl. Phys. **A193** (1972) 647.

[10] N. Fröman and P. O. Fröman, JWKB Approximation (North-Holland, Amsterdam, 1965) chap. 9, sect. 1, pp. 92–97.

[11] S. G. Nilsson, J. R. Nix, A. Sobiczewski, Z. Szymański, S. Wycech, C. Gustafson, and P. Möller, Nucl. Phys. **A115** (1968) 545.

[12] M. Brack, J. Damgaard, A. S. Jensen, H. C. Pauli, V. M. Strutinsky, and C. Y. Wong, Rev. Mod. Phys. **44** (1972) 185.

[13] J. R. Nix, Ann. Rev. Nucl. Sci. **22** (1972) 65.

[14] P. Möller, G. A. Leander, and J. R. Nix, Z. Phys. **A323** (1986) 41.

[15] P. Möller and J. R. Nix, Atomic Data Nucl. Data Tables **26** (1981) 165.

[16] R. Bengtsson, P. Möller, J. R. Nix, and Jing-ye Zhang, Phys. Scr. **29** (1984) 402.

[17] K. Böning, Z. Patyk, A. Sobiczewski, and S. Ćwiok, Z. Phys. **A325** (1986) 479.

[18] P. Armbruster, Ann. Rev. Nucl. Part. Sci. **35** (1985) 135.

[19] G. Münzenberg, Rep. Prog. Phys. **51** (1988) 57.

[20] S. Hofmann, N. Ninov, F. P. Heßberger, P. Armbruster, H. Folger, G. Münzenberg, H. J. Schött, A. G. Popeko, A. V. Yeremin, A. N. Andreyev, S. Saro, R. Janik, and M. Leino, Z. Phys. **A 350** (1995) 277.

[21] S. Hofmann, N. Ninov, F. P. Heßberger, P. Armbruster, H. Folger, G. Münzenberg, H. J. Schött, A. G. Popeko, A. V. Yeremin, A. N. Andreyev, S. Saro, R. Janik, and M. Leino, Z. Phys. **A 350** (1995) 281.

[22] S. Hofmann, N. Ninov, F. P. Heßberger, P. Armbruster, H. Folger, G. Münzenberg, H. J. Schött, A. G. Popeko, A. V. Yeremin, A. N. Andreyev, S. Saro, R. Janik, and M. Leino, GSI Nachrichten, 11-94, Nov 1994 and to be published.

[23] P. Möller, J. R. Nix, W. D. Myers, and W. J. Swiatecki, Atomic Data Nucl. Data Tables (1994) to be published.

[24] P. Möller, J. R. Nix, and K.-L. Kratz, Atomic Data Nucl. Data Tables (1995) to be published.

[25] Y. Aboussir, J. M. Pearson, A. K. Dutta, and F. Tondeur, Nucl. Phys. **A549** (1992) 155.

[26] X.-L. Han, C.-L. Wu, D. H. Feng, and M. W. Guidry, Phys. Rev. **C45** (1992) 1127.

[27] Yu. A. Lazarev, Yu. V. Lobanov, Yu. T. Oganessian, F. Sh. Abdullin, V. K. Utyonkov, G. V. Buklanov, B. N. Gikal, S. Iliev, A. N. Mezentsev, A. N. Polyakov, I. M. Sedykh, I. V. Shirokovsky, V. G. Subbotin, A. M. Sukhov, Yu. S. Tsyganov, V. E. Zhuchko, R. W. Lougheed, K. J. Moody, J. F. Wild, E. K. Hulet, and J. H. McQuaid, Phys. Rev. Lett. **73** (1994) 624.

[28] P. Armbruster, J. Phys. Soc. Jpn. **58** (1989) Suppl. p. 239.